Hematopoietic reconstitution by multipotent adult progenitor cells: precursors to long-term hematopoietic stem cells

Marta Serafini,[1] Scott J. Dylla,[3] Masayuki Oki,[1] Yves Heremans,[1] Jakub Tolar,[2] Yuehua Jiang,[1] Shannon M. Buckley,[1,4] Beatriz Pelacho,[1] Terry C. Burns,[1] Sarah Frommer,[1] Derrick J. Rossi,[3] David Bryder,[3] Angela Panoskaltsis-Mortari,[2] Matthew J. O'Shaughnessy,[2] Molly Nelson-Holte,[1,4] Gabriel C. Fine,[1] Irving L. Weissman,[3] Bruce R. Blazar,[2] and Catherine M. Verfaillie[1,4]

[1]Stem Cell Institute and [2]Cancer Center and Department of Pediatrics, Division of Hematology, Oncology, Blood and Marrow Transplant Program, University of Minnesota, Minneapolis, MN 55455
[3]Department of Pathology, Institute for Stem Cell Biology and Regenerative Medicine, Stanford University School of Medicine, Stanford, CA 94305
[4]Department of Medicine, Stamcel Instituut Leuven, Katholieke Universiteit Leuven, Leuven 3000, Belgium

For decades, in vitro expansion of transplantable hematopoietic stem cells (HSCs) has been an elusive goal. Here, we demonstrate that multipotent adult progenitor cells (MAPCs), isolated from green fluorescent protein (GFP)–transgenic mice and expanded in vitro for >40–80 population doublings, are capable of multilineage hematopoietic engraftment of immunodeficient mice. Among MAPC-derived GFP$^+$CD45.2$^+$ cells in the bone marrow of engrafted mice, HSCs were present that could radioprotect and reconstitute multilineage hematopoiesis in secondary and tertiary recipients, as well as myeloid and lymphoid hematopoietic progenitor subsets and functional GFP$^+$ MAPC-derived lymphocytes that were functional. Although hematopoietic contribution by MAPCs was comparable to control KTLS HSCs, approximately 10^3-fold more MAPCs were required for efficient engraftment. Because GFP$^+$ host-derived CD45.1$^+$ cells were not observed, fusion is not likely to account for the generation of HSCs by MAPCs.

CORRESPONDENCE
Catherine M. Verfaillie:
catherine.verfaillie@med.kuleuven.be

Abbreviations used: eGFP, enhanced GFP; ESC, embryonic stem cell; GVHD, graft-versus-host disease; HSC, hematopoietic stem cell; LT-HSC, long-term repopulating HSC; MAPC, multipotent adult progenitor cell; mESC, mouse ESC; NOD, nonobese diabetic; PB, peripheral blood.

Hematopoietic stem cells (HSCs) reside predominantly in the BM and can be purified to near homogeneity based on their c-Kit$^+$, Thy1.1^{low}, hematopoietic lineage marker negative (Lin$^-$), Sca-1$^+$ phenotype; i.e., KTLS cells (1, 2). HSCs efficiently repopulate the hematopoietic system of primary recipients, and purified donor-derived KTLS cells from engrafted mice robustly reconstitute secondary hosts. The ability to expand or generate HSCs ex vivo would greatly facilitate the development of novel therapies for hematopoietic disorders for which no current therapy exists, or where numbers of available HSCs are insufficient. Although improvement of in vitro HSC expansion or generation of HSCs from embryonic stem cells (ESCs) might provide a solution, both are at early stages of research. Furthermore, for ESC-derived HSCs to be safe in transplantations, they must be free of residual teratogenic cells (3–6). Aside from HSCs, the BM contains at least one other multipotent stem cell population, mesenchymal stem cells. The contribution of HSCs is restricted to hematopoietic cells, whereas mesenchymal stem cells appear limited to muscle, cartilage, bone, and fat differentiation (7, 8). Although rare cells have been postulated to contribute to both hematopoietic and nonhematopoietic cells, "donor-derived" tissues often express both donor and host markers (9–14).

Recently, numerous groups have isolated nonhematopoietic cell populations from the BM or umbilical cord blood via in vitro culture, which appear able to differentiate into cells with mesodermal, endodermal, and ectodermal characteristics (15–17). In previously published studies, we demonstrated that it was possible to isolate a clonal population of cells, named

M. Serafini and S.J. Dylla contributed equally to this work.
The online version of this article contains supplemental material.

multipotent adult progenitor cells (MAPCs), from murine BM that contributes to all three germ layers upon injection into blastocysts (18, 19). MAPCs differentiate into various lineages in vitro using defined cytokine combinations, and when transplanted into sublethally irradiated nonobese diabetic (NOD)-SCID mice, they contribute at low levels to hematopoietic and some endodermal tissues (19). Reyes et al. (20) recently reported that MAPC-like cells can be transferred from donor to host after whole BM transplantation, potentially explaining the plasticity of many BM-derived populations (12, 21, 22).

Since the initial description of MAPCs, we improved MAPC isolation and expansion conditions (23). MAPC clones isolated using improved protocols express Oct4 (a transcription factor required for undifferentiated ESC maintenance; reference 24) at levels approaching those of ESCs. However, MAPCs do not express two other transcription factors known to play a major role in ESC pluripotency, Nanog and Sox2 (25–27). These Oct4-expressing MAPCs differentiate more robustly in vitro to mesodermal and endodermal cell types as compared with MAPCs described previously (unpublished data). Here, we demonstrate that MAPC populations contribute to hematopoiesis in vivo and may precede HSCs in ontogeny given that they generate long-term repopulating HSCs (LT-HSCs) and the full repertoire of hematopoietic progenitors.

RESULTS

Characteristics of Oct4^{high} MAPCs

MAPCs were derived under low oxygen (O_2) conditions (23) from the BM of two independent C57BL mouse strains that express enhanced GFP (eGFP) under control of the β-actin promoter. Only MAPC clones that expressed Oct4 at levels ≥20% of the R1 murine ESC line and stained positive with an anti-Oct4 antibody (Fig. S1, available at http://www.jem.org/cgi/content/full/jem.20061115/DC1) were used for subsequent studies. Because Oct4 levels vary upon long-term passage, cell aliquots were analyzed for *Oct4* mRNA expression at the time of transplantation (Table S1). Phenotypically, MAPCs were CD31, CD44, CD45, CD105, Thy1.1, Sca-1, E-cadherin, MHC class I and II, as well as hematopoietic lineage marker negative, and expressed low levels of EpCAM and high levels of c-Kit, VLA-6, and CD9 (Fig. S2). Furthermore, low O_2-derived MAPCs did not express detectable transcripts of the hematopoietic-specific transcription factors *Lmo2*, *Scl*, *Gata2*, *Ikaros*, or *Pu.1*.

Long-term multilineage hematopoietic repopulating activity of MAPCs

Initial attempts to transplant 10^6 MAPCs into lethally irradiated C57BL mice failed due to pancytopenia. We next transplanted MAPCs into sublethally irradiated NOD-SCID mice that also received anti–asialo-GM1 antibodies to deplete recipient NK cells (28). 3 wk after transplantation of 0.3–1 × 10^6 MAPCs, ∼5% GFP$^+$CD45.2$^+$ donor cells could be detected in the blood. The percentage of GFP$^+$ cells increased substantially by 6–8 wk and continued to increase until 20 wk after transplantation. Engraftment (≥1% GFP$^+$CD45.2$^+$CD45.1$^-$ cells) was observed in 19/26 and 2/2 mice transplanted with MAPC clone DDD and G6, respectively, 3–21 wk after transplant (Tables I and S1).

MAPCs transplanted in the 21/28 mice that engrafted were <35% hypodiploid or hyperdiploid, and expressed Oct4 mRNA between 13 and 100% of that observed in mouse ESCs (mESCs; Table S1). Of the seven mice that did not show hematopoietic engraftment, two animals received cells that were 95% aneuploid. Of note, animals transplanted with euploid cells or aneuploid cells did not develop tumors with posttransplant follow-up of 21 wk. Furthermore, cytogenetic analysis on peripheral blood (PB) of MAPC-transplanted mice also showed a normal karyotype (Table S3, available at http://www.jem.org/cgi/content/full/jem.20061115/DC1). Of the remaining five animals that were not reconstituted, three received MAPCs that expressed Oct4 mRNA at levels 2% of mESC, and two animals showed no engraftment despite transplantation with 75 and 90% of euploid cells expressing 52 and 55% Oct4 mRNA (vs. mESC), respectively.

Although the degree of hematopoietic contribution from MAPCs varied, chimerism of primary recipients was maintained until mice were killed as late as 24 wk after transplant. GFP$^+$ cells in the BM, spleen, PB, and LNs appropriately expressed markers for B lymphocytes, T lymphocytes, or myeloid cells (Fig. 1). In the spleen and PB of long-term engrafted mice, we also detected GFP$^+$ dendritic cells, NK cells,

Table I. Frequency and degree of reconstitution in primary MAPC-transplanted mice

Frequency and level of reconstitution[a]		
	0.3–1 × 10^6 cells	0.3–1 × 10^5 cells
3–12 wk	12/18 (67%) (1.0–84.4)[b]	ND
13–21 wk	9/10 (90%) (8.1–95.3)[b]	4/11 (36%) (1.9–2.1)[b]

Cells transplanted[c]	Transplanted mice	Positive mice	Positive mice (%)	Engraftment (%)
1 × 10^6	19	15	71	82.5 (69.7–95.3)[b]
3 × 10^5	4	4	100	23.0
1 × 10^5	6	3	50	2.0 (1.9–2.1)[b]
3 × 10^4	5	1	20	1.9

Additional information on engraftment levels and quality control of cells used is detailed in Table S1. ND, not done.

[a]BM of MAPC-reconstituted NOD-SCID mice was analyzed by flow cytometry 3–12 and 13–21 wk after transplant for the presence of GFP$^+$CD45.1$^-$CD45.2$^+$ donor-derived cells. Chimerism was determined as presence of ≥1% GFP$^+$CD45.1$^-$CD45.2$^+$ donor-derived cells in the BM.

[b]Range.

[c]Varying doses of MAPCs were intravenously transplanted into sublethally irradiated NOD-SCID mice. 6–21 wk after transplant, BM was examined for chimerism. Engraftment was defined as ≥1% GFP$^+$CD45.1$^-$CD45.2$^+$ donor-derived cells in the BM. The level of engraftment is the mean of the percentage engraftment for each of the dilutions at the latest time point determined (20–21 wk).

and megakaryocytes (Fig. S3, available at http://www.jem.org/cgi/content/full/jem.20061115/DC1). The majority of GFP$^+$ cells in BM obtained between 3 and 10 wk after transplantation were Mac-1$^+$/Gr-1$^+$ double positive, although B and T lymphocytes could be detected (Fig. S4). Between 11 and 21 wk after MAPC infusion, lymphoid repopulation increased, thereby confirming stable, long-term multilineage reconstitution (Fig. S4).

We next evaluated the fraction of animals that engrafted with lower doses of MAPCs (3×10^4 to 10^6 cells/mouse) to assess the minimal dose of MAPCs required to establish long-term, stable chimerism (Table I). Hematopoietic reconstitution of all lineages was observed in one out of five mice injected with 3×10^4 MAPCs and in three out of six mice injected with 10^5 cells, suggesting that the minimal dose of MAPCs needed for hematopoietic reconstitution is ~50,000 cells.

To directly compare MAPC-based contribution to hematopoiesis with KTLS HSCs, we co-transplanted 600 KTLS cells or 7.5×10^5 MAPCs from β-actin GFP mice with $0.2–1 \times 10^6$ Sca-1–depleted CD45.1$^+$ BM cells in sublethally irradiated NOD-SCID mice. Hematopoietic reconstitution by MAPCs was similar to KTLS cells, and the repertoire of hematopoietic engraftment by MAPCs versus KTLS cells was virtually indistinguishable (Fig. 2).

Several studies have suggested that unexpected contribution of adult stem cells to tissues other than the lineage of origin may be due to fusion of donor cells with host cells (8, 30–32). In all mice analyzed, we never detected CD45.1$^+$CD45.2$^+$ or CD45.1$^+$GFP$^+$ cells, suggesting that fusion between donor (CD45.2$^+$GFP$^+$) MAPCs and recipient (CD45.1$^+$) cells does not contribute to hematopoietic reconstitution (Figs. 1 and 2). CD45.1$^+$GFP^{dim} cells were present in both MAPC and KTLS transplants, but these cells were all Mac1$^+$ and represent host-derived macrophage engulfment of donor-derived GFP$^+$ cells (not depicted).

Self-renewal capacity of MAPC-derived HSCs

Within the GFP$^+$CD45.2$^+$CD45.1$^-$ BM cells of primary recipients, we could detect 1–2% ckit$^+$Sca-1$^+$Lin$^-$ (KLS) and ~0.1% ckit$^+$Lin$^-$Sca-1$^+$Flk2$^-$ (KLSFlk2$^-$) cells. This suggested in vivo generation of LT-HSCs from MAPCs (Fig. 3 A; reference 29).

To determine whether functional LT-HSCs were generated by MAPCs, we evaluated whether MAPC-derived cells from primary recipients could stably reconstitute secondary mice. In an initial set of experiments, 10^6 total BM cells from primary recipients of MAPCs or KTLS cells at 16–20 wk after transplant were transferred to five lethally irradiated NOD-SCID or C57BL-CD45.1$^+$ mice. Three out of five

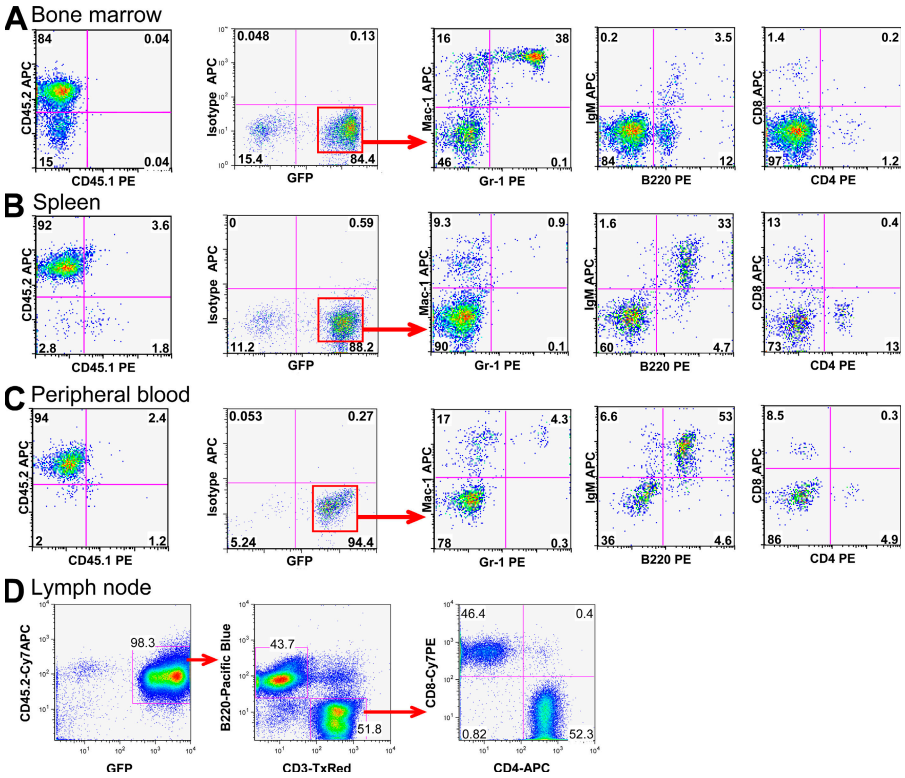

Figure 1. Hematopoietic reconstitution from MAPCs grafted in NOD-SCID mice. 10^6 GFP$^+$CD45.2$^+$ MAPCs were transplanted in sublethally irradiated NOD-SCID mice treated with anti-asialo-GM1 antibodies 4 h before transplantation and on days +11 and +22. Representative flow cytometry profiles of BM, spleen, PB, and LNs of NOD-SCID (CD45.1$^+$) mice ≥12 wk after transplant demonstrating multilineage (B lymphoid, T lymphoid, and myeloid cells) reconstitution. Contour plots shown are after gating on GFP fraction, as indicated.

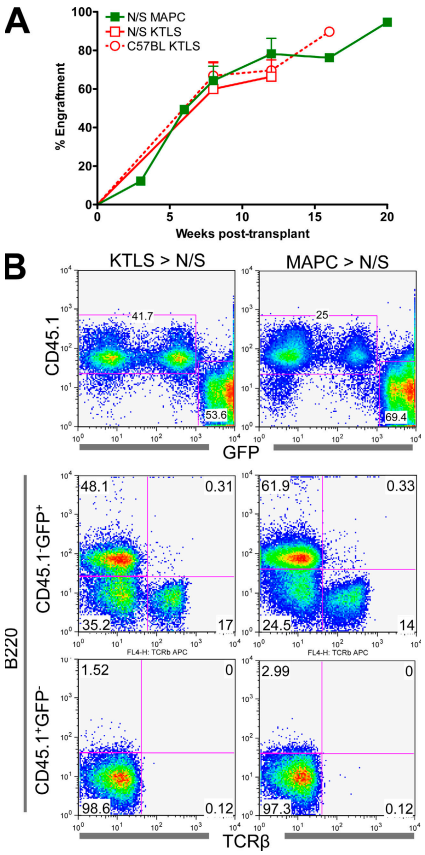

Figure 2. Hematopoietic reconstitution from KTLS HSCs versus MAPCs. 2–3 × 10^5 Sca-1–depleted, host-derived BM cells were co-transplanted with 600 KTLS or 0.75 × 10^6 MAPCs from eGFP$^+$CD45.2$^+$ donor mice into sublethally irradiated NOD-SCID (N/S) or C57BL-CD45.1$^+$ recipients. (A) Mice were evaluated at intermittent time points for PB eGFP$^+$CD45.2$^+$ cells. (B) Representative multilineage reconstitution of KTLS- versus MAPC-engrafted NOD-SCID mice at week 12.

NOD-SCID and three out of five C57BL mice that received BM from MAPC-engrafted mice, and two out of five NOD-SCID and five out of five C57BL mice transplanted with KTLS progeny survived to week 8 after transplantation. All surviving secondary mice had high levels of GFP$^+$CD45.2$^+$ multilineage hematopoiesis at 24 wk after transplant (Fig. 3 B). Furthermore, similar levels of donor-derived LT-HSCs (KLS Flk2$^-$CD34$^-$) and all hematopoietic progenitor populations were present in the BM of C57BL secondary recipients of KTLS- and MAPC-derived BM cells (Table II and Table S5, which is available at http://www.jem.org/cgi/content/full/jem.20061115/DC1; reference 30). Similar results were observed in a second experiment where total mononuclear cells (10^6 cells/mouse, $n = 6$) and CD45$^+$ selected cells (10^6 cells/mouse, $n = 9$) were transplanted from a primary MAPC-engrafted recipient, and long-term GFP$^+$CD45.2$^+$ hematopoietic reconstitution was detected in secondary recipients (Table III).

To more clearly demonstrate that MAPCs generate LT-HSCs, we isolated GFP$^+$KTLS cells from MAPC-engrafted animals and transplanted these into secondary recipients. Co-transplantation of 200 GFP$^+$KTLS cells with 10^6 Sca-1–depleted BM cells into lethally irradiated mice resulted in the establishment of long-term GFP$^+$ hematopoiesis in three out of four NOD-SCID and four out of four C57BL mice (Table III). We further established the generation of functional MAPC-derived HSCs and their downstream progenitors by demonstrating that these cells could both radioprotect and establish long-term hematopoiesis. To do this, we transplanted 2 × 10^3 GFP$^+$ KLS cells without Sca-1–depleted cells. This resulted in robust GFP$^+$CD45.2$^+$ hematopoietic reconstitution in two out of three mice, and multilineage reconstitution

Table II. MAPC contribution to hematopoietic stem and progenitor populations in secondary recipients

	Source of primary BM	
Population	KTLS	MAPCs
LT-HSC	69.6 ± 12%	64.6 ± 27%
CLP	56.9 ± 9%	57.4 ± 18%
CMP	63.5 ± 21%	37.4 ± 27%
GMP	64.3 ± 22%	38.9 ± 30%
MEP	62.5 ± 21%	36.4 ± 27%

0.75 × 10^6 eGFP MAPCs were transplanted into lethally irradiated NOD-SCID mice with 2 × 10^5 Sca-1–depleted cells of host origin. 20 wk after transplant, 10^6 BM cells were serially transplanted into lethally irradiated C57BL-CD45.1$^+$ hosts. At week 24, BM was harvested and assessed for primary donor (eGFP$^+$CD45.2$^+$) contribution to LT-HSCs (KLSFlk2$^-$CD34$^-$), common lymphoid progenitors (CLP; Lin$^-$ckit^{low}Sca-1^{low}IL7Rα$^+$Flk2$^+$), common myeloid progenitors (CMP; Lin$^-$ckit$^+$Sca-1$^-$CD16/32^{low}CD34$^+$), granulocyte macrophage progenitors (GMP; Lin$^-$ckit$^+$Sca-1$^-$CD16/32$^+$CD34$^+$), and megakaryocyte erythrocyte progenitors (MEP; Lin$^-$ckit$^+$Sca-1$^-$CD16/32^{low}CD34$^-$). Data for $n \geq 3$ mice per group is shown.

Table III. Frequency and degree of reconstitution in secondary transplants

Cell type	Host strain	Total MNC (1 ×10^6)	CD45$^+$ (1 ×10^6)	KLS (2 × 10^3)	KTLS (2 × 10^2)
MAPCs	NOD-SCID	[a]3/3 (100%) (13.3–73.7)[b]	5/5 (100%) (0.4–10)[b]	ND	[a]3/4 (75%) (0.8–16.4)[b]
	C57BL	[a]3/3 (100%) (15.1–90.7)[b]	[a]3/4 (75%) (3.8–94.8)[b]	[a]2/3 (67%) (83.0–89.5)[b]	[a]4/4 (100%) (17.5–30.1)[b]
KTLS	NOD-SCID	[c]2/2 (100%) (1.7–7.5%)[b]	ND	ND	ND
	C57BL	5/5 (100%) (9–77.3%)[b]	ND	ND	ND

Secondary transplants were performed using cells from GFP$^+$ MAPC- or GFP$^+$ KTLS-grafted primary mice 16–21 wk after transplantation. Total mononuclear cells (MNC) from the BM of primary NOD-SCID or C57BL recipients, and cells enriched for CD45$^+$, GFP$^+$Lin$^-$Sca-1$^+$c-kit$^+$ (KLS), or GFP$^+$Lin$^-$Sca-1$^+$c-kit$^+$Thy-1^{lo} (KTLS) cells were transplanted intravenously into lethally irradiated NOD-SCID or wild-type C57BL-CD45.1$^+$ mice (five recipient animals for each strain). KTLS populations in secondary transfers were co-transplanted with 10^6 Sca-1–depleted BM cells from mice of host background. Animals were killed 15–24 wk after transplantation, and engraftment levels were determined in the BM as the presence of GFP$^+$CD45.1$^-$CD45.2$^+$ donor-derived cells. The percentage of mice engrafted and chimerism ranges are shown. ND, not done.

[a]Wherever the numerator was <5, mice had died due to radiation sickness.

[b]Range.

[c]Blood chimerism at week 8. Mice died at week 10 due to illness.

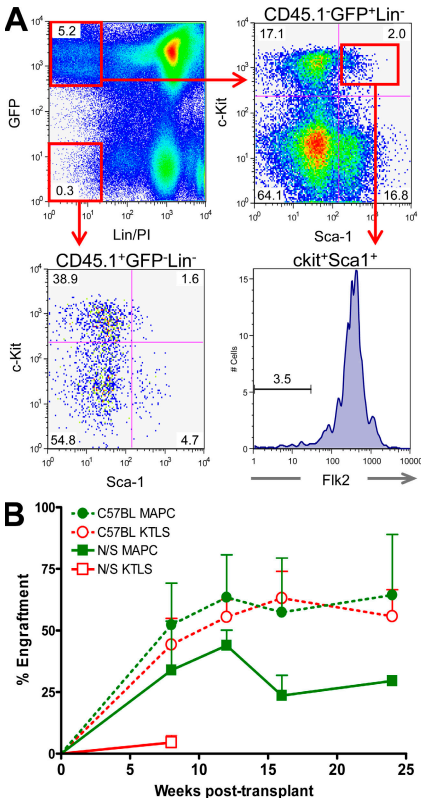

Figure 3. MAPCs generate KLS Flk2$^-$ HSCs and engraft secondary recipients. 0.75 × 10^6 eGFP MAPCs were transplanted into lethally irradiated NOD-SCID mice with 2 × 10^5 Sca-1–depleted cells of host origin. 20 wk after transplant, 10^6 BM cells were serially transplanted into lethally irradiated NOD-SCID or C57BL-CD45.1$^+$ hosts. (A) 20 wk after transplant, MAPC-engrafted animals were killed and BM was evaluated for the presence of eGFP$^+$CD45.2$^+$ hematopoietic stem and progenitor cells. (B) PB was obtained periodically to assess primary donor (eGFP$^+$CD45.2$^+$) contribution and multilineage (T cell, B cell, and myeloid) engraftment.

that persisted in all secondary recipients until they were killed at weeks 15–24 (Table III).

BM obtained 16 wk after transplant from secondary recipients that received 2 × 10^3 MAPC-derived GFP$^+$ KLS cells contained 0.8–1.3% GFP$^+$ KLS cells (not depicted). When 10^6 total BM cells from these secondary recipients were transplanted in 10 lethally irradiated tertiary C57BL mice, 4–37% GFP$^+$CD45.2$^+$ chimerism was seen in the seven tertiary surviving mice 1 mo after transplantation. At 3 mo, two out of seven animals showed GFP$^+$CD45.2$^+$ chimerism (2.7 and 70%), but engraftment was skewed toward the myeloid lineage. In a separate experiment, of the three NOD-SCID mice that received 10^6 BM cells from secondary mice that had received total BM cells from primary MAPC- or KTLS-grafted animals, two out of five KTLS- and one out of five MAPC-derived tertiary recipients remained alive 3 mo after transplant, with multilineage chimerism levels of 8 ± 0.9% and 11.5% in surviving mice, respectively.

Immune reconstitution by MAPC-derived hematopoietic cells

That MAPCs generate lymphoid cells was first observed using intravital microscopy, demonstrating obvious GFP fluorescence in all lymphoid organs, including the thymus, spleen, and LNs (Fig. 4 A). This was confirmed by flow cytometry, where mature B and T lymphocytes were detected in all organs analyzed (Figs. 1, 4, and S4). In addition, histopathology of mesenteric LNs demonstrated that MAPC-derived T and B cells can form normal primary follicles (Fig. 4 B).

The thymus of six NOD-SCID mice 6–20 wk after transplant with 10^6 MAPCs were shown to contain 23 ± 16.5 × 10^6 cells (1–50 × 10^6), of which 73 ± 35.3% (5–99%) were GFP$^+$CD45.2$^+$ (Fig. 4 C). GFP$^+$CD45.2$^+$ cells constituted major portions of the double-negative, double-positive, and CD4 and CD8 single-positive populations (Fig. 4 D). Moreover, >50% of single GFP$^+$CD4 or GFP$^+$CD8 T cells expressed the TCR-β, as would be anticipated for mature thymocytes before emigration into the periphery. All four stages of triple-negative thymocytes were also represented (Fig. 4 E). Finally, mature T cells were present in inguinal LNs (Fig. 1).

To test lymphoid cell function, we examined the in vitro response of MAPC-derived CD4/CD8 cells to TCR-CD3/CD28-mediated signals. The level of [^{3}H]thymidine incorporation was similar in splenic T cells from MAPC-engrafted versus control GFP-transgenic mice 3–7 d after stimulation (Fig. 4 F). Serum of NOD-SCID mice not grafted with MAPCs had detectable levels of IgM, but not IgG_2. In contrast, we detected both IgG_2 and IgM in the serum of MAPC-engrafted mice (n = 6), demonstrating normal B and T cell function, as an antibody class switch from IgM to IgG_2 had occurred (Table IV).

Of note, a single animal developed clinical and pathological features indicative of severe chronic graft-versus-host disease (GVHD) 16 wk after transplantation with 0.6 × 10^6 MAPCs. Tissue histopathology showed chronic GVHD of the skin, along with severely damaged bile ducts in the liver and severe lung damage (Fig. 5). In areas of chronic GVHD-induced injury (not depicted), donor T cells were predominantly CD3$^+$CD4$^+$, with lesser numbers of CD3$^+$CD8$^+$ T cells.

Table IV. MAPC-derived B cells undergo antibody class switching

Mouse n	IgG_2 (μg/ml)	IgM (μg/ml)
6	652	284
10	139	381
13	NS	190
14	3,671	310
23	189	205
39	60	495
40	18	226

Murine IgM and IgG_2 levels were measured by ELISA in the serum of NOD-SCID mice 12–21 wk after MAPC transplant. NS, not significant.

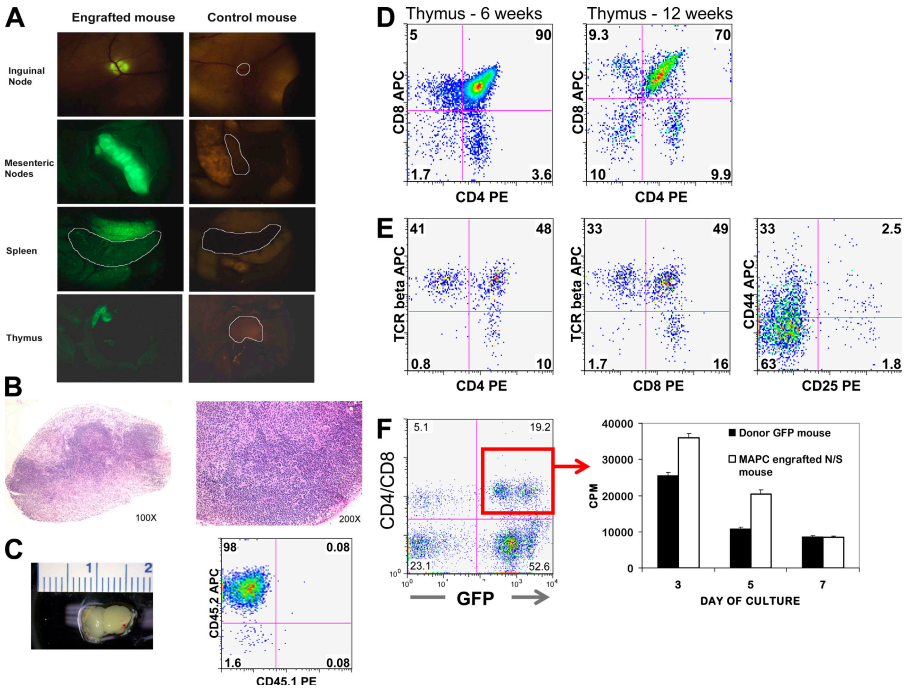

Figure 4. Functional lymphoid reconstitution in MAPC-engrafted animals. Multiparameter analysis was performed to determine the degree of lymphohematopoietic engraftment. (A) Intravital microscopy was performed, demonstrating GFP cells in all lymphoid organs, including the thymus, spleen, and LNs of a NOD-SCID mouse 13 wk after transplantation of 10^6 MAPCs. (B) Hematoxylin and eosin–stained sections of a mesenteric LNs harvested from an MAPC-engrafted NOD-SCID mouse, demonstrating normal primary lymphoid follicles. (C) Representative photograph of the thymus from a NOD-SCID mouse 12 wk after transplant with flow cytometry, demonstrating >95% $GFP^+CD45.2^+$ donor-derived cells in the thymus. Representative thymic engraftment by GFP^+ MAPC-derived cells (D) 6 and 12 wk after transplant followed by (E) TCR-β, CD44, and CD25 expression profiles 12 wk after transplant. (F) At 13 wk, GFP^+ $CD4/CD8^+$ cells were isolated by FACS (95.8% purity) from the spleen of an MAPC-engrafted mouse. After stimulation by anti-CD3/CD28–coated beads, proliferation was assessed by $[^3H]$thymidine incorporation. Control cells were harvested from the spleen of an MAPC donor background $CD45.2^+GFP^+$ animal.

Engraftment in other tissues

We also evaluated engraftment in tissues other than the lymphohematopoietic organs with the primary purpose of assessing extrahematopoietic contribution, and secondarily to investigate whether microscopic tumors were formed. In all sections analyzed, neither microscopic nor macroscopic tumors were observed. All GFP^+ cells in the tissues analyzed from KTLS-transplanted mice were hematopoietic in origin (i.e., $CD45^+$), confirming no extrahematopoietic contribution by HSCs (14). In MAPC-transplanted animals, GFP^+ cells were readily detectable in the brain, muscle, liver, lung, and gut, but the vast majority of these cells were also $CD45^+$. Among the GFP^+ cells that did not co-label with hematopoietic markers, we found no evidence for neural, astrocytic, oligodendrocyte, or epithelial differentiation. The nature of these GFP^+CD45^- cells is currently unclear. In three animals, we detected rare individual GFP^+ cells within the heart that were striated and costained with anti-cardiac troponin-I antibodies (not depicted). The low frequency of this event is consistent with cell fusion (9, 14), although these cells were not detectable in KTLS-transplanted animals. This would suggest that this contribution is specific to MAPCs, but at the moment we cannot speculate on the possible explanation for this phenomenon.

DISCUSSION

In BM, multiple populations of stem and progenitor cells exist with defined potential. The best characterized of these is the HSC, which gives rise to all hematopoietic lineages. Aside from HSCs, BM also contains other multipotent cells, including mesenchymal stem cells. Several recent studies have suggested that more primitive cells may exist in the BM or umbilical cord blood, with differentiation potential toward mesodermal, endodermal, and ectodermal fates, including MAPCs (15–19, 31). Each of these populations is purified using in vitro culture techniques, and it remains to be determined whether they exist in vivo.

We previously demonstrated that clonally derived MAPCs contribute to hematopoiesis in a transplant setting (19). However, contribution was low (2–8%) and progeny were not thoroughly characterized. Here, we show that clonally derived MAPCs functionally reconstitute the hematopoietic system in vivo and generate HSCs and their progenitor cell populations, which robustly contribute to multilineage engraftment in primary and secondary irradiated recipients. MAPCs alone were not radioprotective, despite the fact that the hematopoietic progeny they generated in vivo are radioprotective. Thus, undifferentiated MAPCs cannot be used

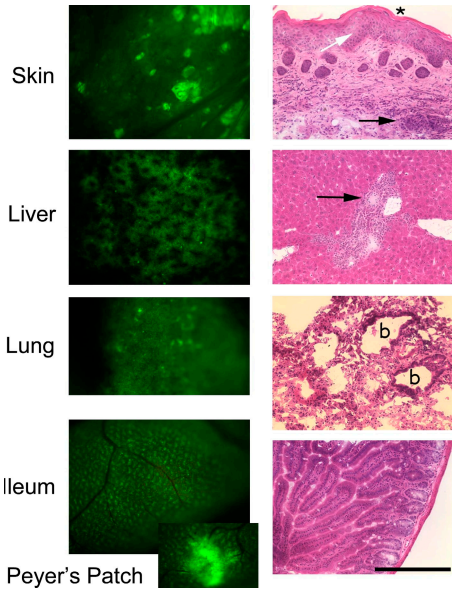

Figure 5. MAPC-engrafted mouse with chronic GVHD. Intravital microscopy and histopathological findings in one NOD-SCID mouse that received 0.6×10^6 MAPCs 16 wk earlier are consistent with the development of chronic GVHD. Left panels show the presence of GFP^+ cells in the GVHD target organs, specifically skin (underlayer), liver, lung, and ileum. All intravital images were taken at a zoom factor of 8× and a transfer lens of 0.63× with an MZFLIII stereomicroscope (300 millisecond exposure). Right panels show the corresponding hematoxylin and eosin stains of cryosections taken from the same mouse (bar, 900 μm). The skin shows inflammation in the dermis and subdermis (black arrow), extensive epidermal hyperplasia (white arrow), and dyskeratosis (asterisk). GVHD score, 3.5 (0–4 scale). The liver has moderate inflammation around the portal triads with evidence of bile duct degeneration (black arrow). GVHD score, 3.0. The lung has peribronchiolar inflammation (b, bronchiole) and extensive parenchymal inflammation in surrounding areas with organizing alveolitis and fibrosis. GVHD score, 4.0. The ileum shows only mild inflammation of the lamina propria as is typical for chronic GVHD. GVHD score, 0.5.

for transplantation as the sole source of hematopoiesis in lethally irradiated recipients, but can reconstitute long-term hematopoiesis. Consistent with the high levels of hematopoietic reconstitution by MAPCs, we could detect GFP^+ cells in all organs analyzed, although most GFP^+ cells coexpressed CD45. Expression of tissue-specific markers in GFP^+ cells was only observed in the heart. The low frequency of this event, and fusogenic properties of cardiac muscle fibers, suggests that this may result from fusion (9, 14). In other tissues, rare GFP^+ cells that did not co-label with hematopoietic markers also did not stain with antibodies against tissue-specific proteins. The nature of these is currently under investigation.

Arguably, hematopoietic engraftment cannot be explained by contamination of the graft by HSCs, as MAPCs were expanded for 40–80 population doublings over 3–5 mo in vitro. If rare contaminating HSCs were responsible for the results observed here, HSC expansion for this period of time and to a level of $>10^8$–10^{12}-fold would be unprecedented for an in vitro culture system. Moreover, MAPCs are derived from BM depleted of $CD45^+$ cells, do not express detectable CD45, Sca-1, Thy1.1, Mac1, Gr1, CD3, CD4, CD8, B220, and Ter119, and do not express HSC-specific transcription factors *Scl*, *Lmo2*, *Gata2*, *Ikaros*, and *Pu.1* (quantitative RT-PCR and gene array analysis [data are available in the GEO database under accession numbers GSE5947 and GSE6291]; not depicted).

Although several studies initially suggested that adult BM stem cells may be capable of acquiring a lineage fate different from the tissue of origin in vivo, several studies have now demonstrated that such plasticity is not cell autonomous but due to fusion between BM-derived cells and cells in the target organ (9, 10, 13, 32, 33). Fusion events characteristically occur infrequently and do not significantly contribute to tissue unless the fused cell has a proliferative or survival advantage over nonfused cells (10). Furthermore, fused cells usually express some markers of both the host and donor cell. To address whether fusion might explain our observations, we used CD45-congenic animals in addition to using donor cells universally expressing GFP. In no instance did we observe coexpression of CD45.1 with CD45.2 or GFP, except in the case of host $Mac1^+GFP^{dim}$ cells that represent host macrophage engulfment of donor-derived cells (Fig. 2 B), making the high level of hematopoietic reconstitution observed after MAPC engraftment extremely unlikely due to fusion.

Numerous advances in MAPC isolation, culture, and transplantation likely explain the significantly greater hematopoietic reconstitution observed after transplantation in this study versus our previous attempts (19). First, we conditioned sublethally irradiated NOD-SCID mice with an anti–NK cell antibody. Although NOD-SCID mice do not have functional B or T cells, they do have robust NK cell activity, which mediates rejection of grafted cells (34). For instance, engraftment levels of human SCID-repopulating cells are significantly enhanced when human $CD34^+$ cells are transplanted in NOD-SCID-IL2Rγc$^{-/-}$ or NOD-SCID-β2M$^{-/-}$ mice, or NOD-SCID mice treated with an anti-CD122 antibody (34). We recently showed that a substantial fraction of murine MAPCs, which are MHC class I low, are rejected early after transplantation in NK-competent animals, leading to significantly lower levels of long-term engraftment compared with transplantation into NK-deficient animals (28). Murine ESC-derived HSCs, which, like MAPCs, are MHC class I low, also yield significantly higher levels of hematopoietic engraftment when transplanted into animals that are NK deficient (4).

Second, MAPCs used in this study were derived using improved methodology (23). Compared with previously generated MAPCs, those derived using 5% O_2 express $\sim 10^3$-fold higher mRNA levels of the ESC-specific transcription factor Oct4 (24). We have evidence that the higher level of Oct4 transcripts is associated with a significantly broader and more robust differentiation ability of MAPCs to several mesodermal and endodermal lineages in vitro (unpublished data).

Not surprisingly, MAPCs were unable to radioprotect lethally irradiated C57BL mice and require co-transplantation of Sca-1–depleted BM to prevent death from pancytopenia early after transplantation. Because myeloid reconstitution is delayed upon transplant of highly purified HSCs into lethally irradiated mice, it is well established that co-transplantation of Sca-1–depleted BM cells is needed to transiently protect animals until mature blood lineages develop (35). The notion that MAPCs are unable to radioprotect is consistent with the hypothesis that MAPCs precede HSCs during ontogeny, and that commitment to an HSC fate might be required before establishing hematopoiesis. The presence of KLS Flk2$^-$ cells (29), robust engraftment of secondary recipients by MAPC-derived GFP$^+$ KTLS, and radioprotection as well as long-term hematopoietic reconstitution by GFP$^+$ KLS cells demonstrates that LT-HSCs are, in fact, generated by MAPCs.

Compared with freshly isolated KTLS cells, significantly more MAPCs are required to establish hematopoiesis. This incongruity likely reflects several differences between the two cell types. First, it is possible that the efficiency of MAPC commitment to LT-HSCs is poor. Second, and most notably, the efficiency of MAPC homing and engraftment in BM niches is, as yet, unknown. In contrast to KTLS cells, MAPCs, aside from *Tie2* (36), do not express *Cxcr4*, *Itga4* and *Itga5*, *Pecam1*, *Cd44*, or *Cd164* (gene array analysis [data are available in the GEO database under accession numbers GSE5947 and GSE6291]; not depicted and references 37–41). This constellation of chemokine and adhesion receptors is known to play a critical role in HSC homing and engraftment, and its absence may contribute to the lower engraftment efficiency of MAPCs versus KTLS cells.

Nevertheless, MAPC-derived progenitors were capable of migrating to the thymus, where they underwent typical differentiation processes as demonstrated by intravital microscopy, flow cytometry, and tissue immunohistochemistry. Peripheral B and T cell reconstitution of the spleen and LNs was intact. Serum Ig levels and IgG_{2a} isotype switching were indicative of successful B cell–T cell interactions. In vitro T cell responses to CD3 and CD28 signals were intact, and in one mouse, donor T cells were sufficiently mature to mount a chronic GVHD response as confirmed by clinicopathological analysis and the presence of mature T cells in GVHD target organs. We do not know the inciting factors for chronic GVHD development in this mouse, but possibilities include failed thymic negative selection, inadequate peripheral tolerance mechanisms, and/or the presence of a pathogen (e.g. virus) that might break existing tolerance. Future studies measuring in vivo responses to foreign antigens will be required to quantify the extent of functional B and T cell responses. Nonetheless, these data demonstrate the capacity of MAPC-derived HSCs to reconstitute irradiated recipients with a functional lymphoid system.

In conclusion, we demonstrate that MAPC cultures can robustly contribute to hematopoiesis in vivo while generating functional lymphoid cells and serially transplantable HSCs, but they do not generate observable microscopic or macroscopic tumors, an important trait when considering their therapeutic utility. Because MAPCs can be expanded for prolonged periods ex vivo without evidence of senescence and can be easily genetically manipulated, they may prove invaluable for the treatment of inherited hematopoietic disorders. Given that MAPCs can differentiate to mesoderm, endoderm, and ectoderm in vitro (42–44), and to the extent that they may be better adapted to do so in vivo given the proper environment, MAPCs may greatly facilitate tissue repair in vivo through the establishment of hematopoietic chimerism as a means to induce transplantation tolerance and, therefore, successful transplantation of MAPC-derived tissue-committed cells without immune-mediated rejection (45, 46).

MATERIALS AND METHODS

Mouse strains. Mice carrying the eGFP gene were provided by M. Okabe (Osaka University, Osaka, Japan; C57BL/6TgN(act-EGFP) ObsC14-Yo1-FM1310) and by I.L. Weissman (C57BL/Ka-CD45.2$^+$-eGFP). Both strains use the β-actin promoter to encode for eGFP, and eGFP expression is present in >95% of all tissue cells. NOD/LtSz-*scid*/*scid* (NOD-SCID) and C57BL/6 (CD45.1$^+$) mice were purchased from The Jackson Laboratory. Mouse colonies were established at the University of Minnesota for the C57BL/Ka-CD45.2$^+$-eGFP, C57BL/6TgN(act-EGFP) ObsC14-Yo1-FM131, and NOD-SCID mice. All mice were housed under specific pathogen-free conditions. All protocols involving mice were approved by the Institutional Animal Care and Use Committee at the University of Minnesota and Stanford University.

MAPC culture and characterization. MAPCs were isolated from the BM of C57BL/6TgN (act-EGFP) ObsC14-Yo1-FM131 mice (clone G6) and C57BL/Ka-CD45.2$^+$-eGFP mice (clone DDD), as described previously (19, 23). In brief, BM was plated in DMEM/MCDB (Invitrogen) containing 10 ng/ml EGF (Sigma-Aldrich), PDGF-BB (R&D Systems), and LIF (Chemicon International), 2% FCS (Hyclone), 1× selenium-insulin-transferrin-ethanolamine, 0.2 mg/ml linoleic acid-bovine serum albumin, 0.8 mg/ml bovine serum albumin (all from Sigma-Aldrich), 1× chemically defined lipid concentrate (Invitrogen), and 1× α-mercaptoethanol (Invitrogen) in a humidified 5% O_2 and 6% CO_2 incubator. After 4 wk, CD45$^+$ and Ter119$^+$ cells were depleted using a MACS separation CS column (Miltenyi Biotec) and plated at 10 cells/well. Clones consisting of cells with Oct4 mRNA levels >20% of mESC (R1 cells, maintained on murine embryonic fibroblasts) were expanded and used for the studies described.

Approximately monthly, MAPCs were analyzed by FACS for cell surface phenotype. Samples were stained with the following fluorochrome-conjugated antibodies: Sca-1 (E13-161.7); c-kit (2B8); Thy1.1 (OX-7); CD44 (IM7); MHC-I^b (H2^b, AF6-88.5); MHC-II^b (IA^b, AF6-120.1); CD31 (MEC13.3); CD3 (145-2C11); B220 (RA3-6B2); Mac1 (M1/70); Gr-1 (8C5); and isotype-PE and APC antibodies. For CD45.2 (104) and CD9 (KMC8) staining, a biotinylated antibody was used, followed by streptavidin and APC. Cells were stained with purified antibody against E-cadherin (ECCD-2; Takara Bio Inc.); EpCAM (G8.8); CD105 (MJ7/18); and CD49f (G0H3). An APC-conjugated goat anti–rat IgG F(ab')$_2$ antibody (Jackson ImmunoResearch Laboratories) was used as secondary antibody. All antibodies were from BD Biosciences unless otherwise noted.

Within 1 wk of transplantation, *Oct4* transcripts and/or Oct4 protein levels were evaluated by quantitative RT-PCR and immunoperoxidase staining, respectively (for primers see Table S2). Transcript levels for the hematopoietic transcription factors *Gata-2*, *Scl*, *Lmo2*, *Pu.1*, and *Ikaros* were evaluated by quantitative RT-PCR (for primers see Table S2). MAPCs were subjected within 1 wk before transplantation to cytogenetic analysis as described previously (23). Results of quantitative RT-PCR for *Oct4* and

cytogenetic analysis of cells used in the studies described are provided in Table S1.

Intermittently, cells were subjected to trilineage (endothelium, hepatocyte, and neuroectodermal) differentiation to prove multipotency of the cell populations used (19, 42). Differentiation was confirmed when transcript levels for *Sox-1*, *Otx-1*, *nestin*, and *NF200* increased at least 50-fold, reaching levels 50–500% of those measured in embryonic mouse brain RNA (for primers see Table S1).

KTLS cell isolation. KTLS (ckit$^+$Sca-1$^+$Thy1.1$^{int/low}$Lin$^-$) cells were isolated as described previously (1)

MAPC and KTLS cell transplantation. For primary grafts, 6–8-wk-old NOD-SCID mice were irradiated with 275 cGy/min at 57 cGy/min. 4 h before injection of MAPCs, NOD-SCID mice were treated with an intraperitoneal injection of anti-asialo GM1 antibody (20 μL of the stock solution diluted in 380 μL of 1× PBS; Wako Chemicals). The injection of anti-asialo GM1 antibody was also performed after transplantation. Transplantation of MAPCs by tail vein injection occurred 12–24 h after irradiation. KTLS cells were transplanted into NOD-SCID mice after irradiation at 350 cGy. Transplantations of MAPCs or KTLS cells into C57BL-CD45.1$^+$ recipients were performed in lethally irradiated (950–1,000 cGy at 57 cGy/min) animals. KTLS cells, and in some instances MAPCs, were co-injected with 2×10^5–10^6 Sca-1/CD3-depleted BM cells of host origin. Blood was obtained at different times after transplantation to assess engraftment.

Secondary and tertiary transplants were performed using 10^6 total BM cells from primary or secondary recipients, respectively. Secondary transplants were also performed using BM CD45$^+$ cells, 2×10^3 cKit$^+$ Sca-1^{low}Lin$^-$GFP$^+$ cells, or 2×10^2 cKit$^+$Sca-1$^+$Thy1.1$^{int/lo}$Lin$^-$GFP$^+$ cells isolated by FACS from primary recipients, the latter combined with 10^6 Sca-1–depleted BM of host background. Cells were either grafted into sublethally irradiated (275–350 cGy) NOD-SCID mice or lethally irradiated (950–1,000 cGy) C57BL-CD45.1$^+$ mice. Blood was obtained at varying times after transplant to follow engraftment. 4–26 wk after transplantation, animals were killed and analyzed for hematopoietic engraftment as described for primary recipients.

Cytogenetic analysis of PB of grafted mice. Cytogenetic analysis was performed as recommended by The Jackson Laboratory (http://www.jax.org/cyto/blood_preps). Three male NOD-SCID mice were transplanted with MAPCs purified from female C57BL/Ka-CD45.2$^+$-eGFP as described above. In brief, 0.2 ml of blood was collected from the retroorbital sinus of primary recipients into heparinized micro-hematocrit tubes. Cells were stimulated by phytohemagglutinine (final concentration, 7.5 mcg/ml; Invitrogen) and lipopolysaccharide (final concentration, 50 mcg/ml; Sigma-Aldrich) for 42.5 h, treated with cholchicine, and harvested, and metaphases were evaluated according to standard cytogenetic techniques.

Flow cytometric analysis of hematopoietic organs of grafted mice. Blood samples were obtained at regular intervals by venipuncture. When the mice were killed, hematopoietic organs (BM, PB, spleen, LNs, and thymus) were harvested, single cell suspensions were prepared, and red blood cells were lysed. Cells were analyzed by flow cytometry for the presence of GFP$^+$ donor-derived leukocytes. For FACS analysis, biotinylated or fluorochrome-conjugated mAbs against the following antigens were used: CD45.2, Thy1.1, c-kit, Sca-1, CD3, B220, Mac-1, Gr1, MHC-II (clones as described above), CD45.1 (A20), CD4 (GK1.5), CD8α (53–6.7), TCRβ (H57-597), TCRγδ (GL3), CD19 (1D3), IgM (II/41), CD41 (MWReg30), CD11c (HL3), CD25 (PC61), CD44 (IM7), IL-7Rα (A7R34), Flk2 (A2F10), and FcγR (CD16/32;2.4G2). GFP$^+$CD45.1$^-$CD45.2$^+$ cells were considered donor in origin, and multilineage engraftment was assessed using the markers described above.

Immunohistochemistry for Oct4 on mouse MAPCs and mouse ESCs (clone R1). Cells were plated at 100 cells/cm^2 and stained with goat anti–Oct-3A/4 polyclonal IgG (Santa Cruz Biotechnology, Inc.) or incubated with goat gamma globulin (Jackson ImmunoResearch Laboratories) as negative control. Biotin SP–conjugated anti–goat IgG (Jackson ImmunoResearch Laboratories) was used as secondary antibody. After the secondary antibody, cells were incubated for 30 min with ABComplex-HRP (DakoCytomation) and developed with DAB$^+$ (DakoCytomation) for 2–5 min.

Analysis of donor cell engraftment in tissues by intravital microscopy. Anesthetized mice (Nembutal) were examined for the presence of GFP$^+$ cells by intravital microscopy as described previously using a stereomicroscope (MZFLIII; Leica) equipped with a GFP2 bandpass filter (Leica) and a Retiga Exi camera with Qcapture software (Qimaging). Exposure times were kept constant for the different organs and, for all mice examined, for objective comparison of GFP fluorescence intensity and any autofluorescence background (47).

Immunological reconstitution. To assess T cell responses in vitro, GFP$^+$CD4$^+$ and GFP$^+$CD8$^+$ cells were isolated from the spleens of an engrafted mouse or a control mouse by FACS. 6×10^4 sorted T cells (ratio for CD4/CD8 is 1:1 in MAPC-grafted mouse and control GFP transgenic mouse) were cultured in 96-well plates with anti-CD3 mAb plus anti-CD28 mAb-coated beads (10^5; provided by C. June and B. Levine, University of Pennsylvania, Philadelphia, PA), and pulsed with tritiated thymidine (1 μCi/well; GE Healthcare) 16–18 h before harvest and counted in the absence of scintillation fluid on a β-plate reader (Packard Instrument Co.). Three individual wells were analyzed per data point.

As an indication of T cell responses in vivo, mice were examined for evidence of GVHD by clinical characteristics (weight loss and appearance) and tissue histopathology using a semiquantitative histopathological scoring system as described previously (48).

IgG and IgM serum levels. Ig levels were determined on serial dilutions of sera by ELISA at the University of Minnesota Cytokine Reference Laboratory as described previously (48).

Engraftment in organs. Transplanted animals were anesthetized and perfused intracardially with 10 ml of 10 mM EDTA/1× PBS, followed by 10 ml Z-Fix (Anatech). Blood was collected before perfusion with PBS and BM between perfusion with PBS and Z-Fix. After systemic perfusion with PBS and Z-Fix, nonhematopoietic organs were removed and post-fixed in Z-Fix for 24 h at 4°C. Fixed tissues were washed with 1× PBS, cryoprotected by overnight incubation in 30% sucrose, quick-frozen in optimum cutting temperature compound, and stored at −80°C. 6-μm cryosections were thaw-mounted onto glass slides and fixed in acetone for 5 min. Spleen, LNs, and thymus were immunostained for donor-derived lymphocytes using anti–CD3-PE, anti–CD4-biotin, rabbit anti–GFP, anti–CD19-PE, anti–CD11b-PE, anti–CD11c-biotin, and anti–CD45.2-biotin (all from BD Biosciences). Biotinylated antibodies were detected with streptavidin-Cy5 (BD Biosciences), and rabbit antibodies were detected with anti–rabbit Alexa 488 (Invitrogen). Stained tissues were analyzed using a confocal microscope (FV500; Olympus) and Fluoview software (version 3.2; Olympus).

Online supplemental material. The online supplemental material contains a more extensive description of the cells transplanted (including phenotype, Oct3a transcript and protein level, and cytogenetics) and the level of engraftment in each individual animal. Additional information is available regarding multilineage reconstitution in the blood, BM, and spleen. Online supplemental material is available at http://www.jem.org/cgi/content/full/jem.20061115/DC1.

We thank M. Blackstadt for help with quantitative RT-PCR; A. Breyers and L. Lien for help with MAPC culture; P. Marker for cell sorting; A. Price and M. Riddle in the B.R. Blazar lab for technical assistance; L. Jerabek for excellent laboratory management;

and D. Bhattacharya and T. Serwold of the I.L. Weissman laboratory for helpful advice and assistance.

The work was supported by DK5829, HL71228, and HL076653 to C.M. Verfaillie; HL52952, HL49997, HL63452, HL073794, and P01 AI 056299 to B.R. Blazar; and HL058770 and AI047457 to I.L. Weissman. S.J. Dylla was supported by an American Cancer Society Edward-Albert Bielfelt Postdoctoral Fellowship (PF-04-087-01-LIB). S. Frommer was supported by National Institutes of Health (NIH) Muscle Training Grant and NIH Musculoskeletal Training Grant (T32AR07612), B. Pelacho was supported by AHA0525748Z, and Y. Heremans was supported by a postdoctoral fellowship from the Juvenile Diabetes Research Foundation.

C.M. Verfaillie has received research funding from Athersys Inc. for work with MAPCs unrelated to the studies in this manuscript. No other authors have conflicting financial interests.

Submitted: 24 May 2006
Accepted: 5 December 2006

REFERENCES

1. Morrison, S.J., and I.L. Weissman. 1994. The long-term repopulating subset of hematopoietic stem cells is deterministic and isolatable by phenotype. *Immunity*. 1:661–673.
2. Ikuta, K., and I.L. Weissman. 1992. Evidence that hematopoietic stem cells express mouse c-kit but do not depend on steel factor for their generation. *Proc. Natl. Acad. Sci. USA*. 89:1502–1506.
3. Sorrentino, B.P. 2004. Clinical strategies for expansion of haematopoietic stem cells. *Nat. Rev. Immunol*. 4:878–888.
4. Kyba, M., R.C. Perlingeiro, and G.Q. Daley. 2002. HoxB4 confers definitive lymphoid-myeloid engraftment potential on embryonic stem cell and yolk sac hematopoietic progenitors. *Cell*. 109:29–37.
5. Wang, L., P. Menendez, F. Shojaei, L. Li, F. Mazurier, J.E. Dick, C. Cerdan, K. Levac, and M. Bhatia. 2005. Generation of hematopoietic repopulating cells from human embryonic stem cells independent of ectopic HOXB4 expression. *J. Exp. Med*. 201:1603–1614.
6. Correia, A.S., S.V. Anisimov, J.Y. Li, and P. Brundin. 2005. Stem cell-based therapy for Parkinson's disease. *Ann. Med*. 37:487–498.
7. Caplan, A.I. 1991. Mesenchymal stem cells. *J. Orthop. Res*. 9:641–650.
8. Prockop, D. 1997. Marrow stromal cells as stem cells for nonhematopoietic tissues. *Science*. 276:71–74.
9. Alvarez-Dolado, M., R. Pardal, J.M. Garcia-Verdugo, J.R. Fike, H.O. Lee, K. Pfeffer, C. Lois, S.J. Morrison, and A. Alvarez-Buylla. 2003. Fusion of bone-marrow-derived cells with Purkinje neurons, cardiomyocytes and hepatocytes. *Nature*. 425:968–973.
10. Wang, X., H. Willenbring, Y. Akkari, Y. Torimaru, M. Foster, M. Al-Dhalimy, E. Lagasse, M. Finegold, S. Olson, and M. Grompe. 2003. Cell fusion is the principal source of bone-marrow-derived hepatocytes. *Nature*. 422:897–901.
11. Kajstura, J., M. Rota, B. Whang, S. Cascapera, T. Hosoda, C. Bearzi, D. Nurzynska, H. Kasahara, E. Zias, M. Bonafe, et al. 2005. Bone marrow cells differentiate in cardiac cell lineages after infarction independently of cell fusion. *Circ. Res*. 96:127–137.
12. Brazelton, T.R., F.M. Rossi, G.I. Keshet, and H.M. Blau. 2000. From marrow to brain: expression of neuronal phenotypes in adult mice. *Science*. 290:1775–1779.
13. Weimann, J.M., C.A. Charlton, T.R. Brazelton, R.C. Hackman, and H.M. Blau. 2003. Contribution of transplanted bone marrow cells to Purkinje neurons in human adult brains. *Proc. Natl. Acad. Sci. USA*. 100:2088–2093.
14. Wagers, A.J., R.I. Sherwood, J.L. Christensen, and I.L. Weissman. 2002. Little evidence for developmental plasticity of adult hematopoietic stem cells. *Science*. 297:2256–2259.
15. D'Ippolito, G., S. Diabira, G.A. Howard, P. Menei, B.A. Roos, and P.C. Schiller. 2004. Marrow-isolated adult multilineage inducible (MIAMI) cells, a unique population of postnatal young and old human cells with extensive expansion and differentiation potential. *J. Cell Sci*. 117:2971–2981.
16. Yoon, Y.S., A. Wecker, L. Heyd, J.S. Park, T. Tkebuchava, K. Kusano, A. Hanley, H. Scadova, G. Qin, D.H. Cha, et al. 2005. Clonally expanded novel multipotent stem cells from human bone marrow regenerate myocardium after myocardial infarction. *J. Clin. Invest*. 115:326–338.
17. Kogler, G., S. Sensken, J.A. Airey, T. Trapp, M. Muschen, N. Feldhahn, S. Liedtke, R.V. Sorg, J. Fischer, C. Rosenbaum, et al. 2004. A new human somatic stem cell from placental cord blood with intrinsic pluripotent differentiation potential. *J. Exp. Med*. 200:123–135.
18. Reyes, M., T. Lund, T. Lenvik, D. Aguiar, L. Koodie, and C.M. Verfaillie. 2001. Purification and ex vivo expansion of postnatal human marrow mesodermal progenitor cells. *Blood*. 98:2615–2625.
19. Jiang, Y., B.N. Jahagirdar, R.L. Reinhardt, R.E. Schwartz, C.D. Keene, X.R. Ortiz-Gonzalez, M. Reyes, T. Lenvik, T. Lund, M. Blackstad, et al. 2002. Pluripotency of mesenchymal stem cells derived from adult marrow. *Nature*. 418:41–49.
20. Reyes, M., S. Li, J. Foraker, E. Kimura, and J.S. Chamberlain. 2005. Donor origin of multipotent adult progenitor cells in radiation chimeras. *Blood*. 106:3646–3649.
21. Krause, D.S., N.D. Theise, M.I. Collector, O. Henegariu, S. Hwang, R. Gardner, S. Neutzel, and S.J. Sharkis. 2001. Multi-organ, multilineage engraftment by a single bone marrow-derived stem cell. *Cell*. 105:369–377.
22. Orlic, D., J. Kajstura, S. Chimenti, I. Jakoniuk, S.M. Anderson, B. Li, J. Pickel, R. McKay, B. Nadal-Ginard, D.M. Bodine, et al. 2001. Bone marrow cells regenerate infarcted myocardium. *Nature*. 410:701–705.
23. Breyer, A., N. Estharabadi, M. Oki, F. Ulloa, M. Nelson-Holte, L. Lien, and Y. Jiang. 2006. Multipotent adult progenitor cell isolation and culture procedures. *Exp. Hematol*. 34:1596–1601.
24. Nichols, J., B. Zevnik, K. Anastassiadis, H. Niwa, D. Klewe-Nebenius, I. Chambers, H. Scholer, and A. Smith. 1998. Formation of pluripotent stem cells in the mammalian embryo depends on the POU transcription factor Oct4. *Cell*. 95:379–391.
25. Chambers, I., D. Colby, M. Robertson, J. Nichols, S. Lee, S. Tweedie, and A. Smith. 2003. Functional expression cloning of Nanog, a pluripotency sustaining factor in embryonic stem cells. *Cell*. 113:643–655.
26. Mitsui, K., Y. Tokuzawa, H. Itoh, K. Segawa, M. Murakami, K. Takahashi, M. Maruyama, M. Maeda, and S. Yamanaka. 2003. The homeoprotein Nanog is required for maintenance of pluripotency in mouse epiblast and ES cells. *Cell*. 113:631–642.
27. Boyer, L.A., T.I. Lee, M.F. Cole, S.E. Johnstone, S.S. Levine, J.P. Zucker, M.G. Guenther, R.M. Kumar, H.L. Murray, R.G. Jenner, et al. 2005. Core transcriptional regulatory circuitry in human embryonic stem cells. *Cell*. 122:947–956.
28. Tolar, J., M.J. O'Shaughnessy, A. Panoskaltsis Mortari, R.T. McElmurry, S. Bell, M. Riddle, R.S. McIvor, S.R. Yant, M.A. Kay, D. Krause, et al. 2006. Host factors that impact the biodistribution and persistence of multipotent adult progenitor cells. *Blood*. 107:4182–4188.
29. Christensen, J.L., and I.L. Weissman. 2001. Flk-2 is a marker in hematopoietic stem cell differentiation: a simple method to isolate long-term stem cells. *Proc. Natl. Acad. Sci. USA*. 98:14541–14546.
30. Akashi, K., D. Traver, T. Miyamoto, and I.L. Weissman. 2000. A clonogenic common myeloid progenitor that gives rise to all myeloid lineages. *Nature*. 404:193–197.
31. Kues, W.A., J.W. Carnwath, and H. Niemann. 2005. From fibroblasts and stem cells: implications for cell therapies and somatic cloning. *Reprod. Fertil. Dev*. 17:125–134.
32. Camargo, F.D., M. Finegold, and M.A. Goodell. 2004. Hematopoietic myelomonocytic cells are the major source of hepatocyte fusion partners. *J. Clin. Invest*. 113:1266–1270.
33. Camargo, F.D., R. Green, Y. Capetenaki, K.A. Jackson, and M.A. Goodell. 2003. Single hematopoietic stem cells generate skeletal muscle through myeloid intermediates. *Nat. Med*. 9:1520–1527.
34. McKenzie, J.L., O.L. Gan, M. Doedens, and J.E. Dick. 2005. Human short-term repopulating stem cells are efficiently detected following intrafemoral transplantation into NOD/SCID recipients depleted of CD122+ cells. *Blood*. 106:1259–1261.
35. Uchida, N., and I.L. Weissman. 1992. Searching for hematopoietic stem cells: evidence that Thy-1.1^{lo} Lin^{-} Sca-1^{+} cells are the only stem cells in C57BL/Ka-Thy-1.1 bone marrow. *J. Exp. Med*. 175:175–184.
36. Arai, F., A. Hirao, M. Ohmura, H. Sato, S. Matsuoka, K. Takubo, K. Ito, G.Y. Koh, and T. Suda. 2004. Tie2/angiopoietin-1 signaling reg-

ulates hematopoietic stem cell quiescence in the bone marrow niche. *Cell*. 118:149–161.
37. Peled, A., I. Petit, O. Kollet, M. Magid, T. Ponomaryov, T. Byk, A. Nagler, H. Ben-Hur, A. Many, L. Shultz, et al. 1999. Dependence of human stem cell engraftment and repopulation of NOD/SCID mice on CXCR4. *Science*. 283:845–848.
38. Papayannopoulou, T. 2000. Mechanisms of stem-/progenitor-cell mobilization: the anti-VLA-4 paradigm. *Semin. Hematol*. 37:11–18.
39. Watt, S., S. Gschmeissner, and P. Bates. 1995. PECAM-1: its expression and function as a cell adhesion molecule on hemopoietic and endothelial cells. *Leuk. Lymphoma*. 17:229–244.
40. Dimitroff, C.J., J.Y. Lee, R.C. Fuhlbrigge, and R. Sackstein. 2000. A distinct glycoform of CD44 is an L-selectin ligand on human hematopoietic cells. *Proc. Natl. Acad. Sci. USA*. 97:13841–13846.
41. Doyonnas, R., J. Yi-Hsin Chan, L.H. Butler, I. Rappold, J.E. Lee-Prudhoe, A.C. Zannettino, P.J. Simmons, H.J. Buhring, J.P. Levesque, and S.M. Watt. 2000. CD164 monoclonal antibodies that block hemopoietic progenitor cell adhesion and proliferation interact with the first mucin domain of the CD164 receptor. *J. Immunol*. 165:840–851.
42. Jiang, Y., D. Henderson, M. Blackstad, A. Chen, R.F. Miller, and C.M. Verfaillie. 2003. Neuroectodermal differentiation from mouse multipotent adult progenitor cells. *Proc. Natl. Acad. Sci. USA*. 100: 11854–11860.
43. Schwartz, R.E., M. Reyes, L. Koodie, Y. Jiang, M. Blackstad, T. Lund, T. Lenvik, S. Johnson, W.S. Hu, and C.M. Verfaillie. 2002. Multipotent adult progenitor cells from bone marrow differentiate into functional hepatocyte-like cells. *J. Clin. Invest*. 109:1291–1302.
44. Reyes, M., A. Dudek, B. Jahagirdar, L. Koodie, P.H. Marker, and C.M. Verfaillie. 2002. Origin of endothelial progenitors in human postnatal bone marrow. *J. Clin. Invest*. 109:337–346.
45. Gandy, K.L., and I.L. Weissman. 1998. Tolerance of allogeneic heart grafts in mice simultaneously reconstituted with purified allogeneic hematopoietic stem cells. *Transplantation*. 65:295–394.
46. Shizuru, J.A., R.S. Negrin, and I.L. Weissman. 2005. Hematopoietic stem and progenitor cells: clinical and preclinical regeneration of the hematolymphoid system. *Annu. Rev. Med*. 56:509–538.
47. Panoskaltsis-Mortari, A., A. Price, J.R. Hermanson, E. Taras, C. Lees, J.S. Serody, and B.R. Blazar. 2004. In vivo imaging of graft-versus-host-disease in mice. *Blood*. 103:3590–3598.
48. Waldschmidt, T.J., A. Panoskaltsis-Mortari, R.T. McElmurry, L.T. Tygrett, P.A. Taylor, and B.R. Blazar. 2002. Abnormal T cell dependent B cell responses in SCID mice receiving allogeneic bone marrow in utero. *Blood*. 100:4557–4564.